A spectroscopic study of the high-redshift Universe

Karman, Wouter

Chapter 1

Introduction

It is nowadays commonly accepted that the Universe started with something called the Big Bang. However, what happened between the Big Bang and now is still largely unknown and has many mysteries for astronomers. Since astronomers like Edwin Hubble discovered in the 1920's that there are many more galaxies beyond our own Milky Way (Hubble 1929), the number of studies of these extragalactic sources has expanded rapidly. The first studies started with classifying the shapes and colours of these sources leading to the famous Hubble Sequence (e.g. Hubble 1926; Morgan 1958; de Vaucouleurs 1959; Sandage 1961). Nowadays, studies search for the first galaxies and stars to have formed in the Universe.

The classification of galaxies according to their morphology was one of the first attempts to understand the evolutionary sequence of galaxies. Hubble classified elliptical galaxies as early type and spiral galaxies as late type, as he thought elliptical galaxies would evolve into large disk structures because of the old age of their stellar populations (Hubble 1936). We now understand that the spiral structure is often destroyed by gravitational instabilities from either inside the galaxy or by external factors such as merging galaxies.

Another classification scheme that is currently widespread is based on the number of stars that are forming in a galaxy. This is based on the discovery that galaxies of a specific mass show a relatively narrow range of star formation rates, and these are called galaxies on the main sequence of star formation (e.g. Noeske et al. 2007; Elbaz et al. 2011). In addition, there are galaxies that are found to have star formation orders of magnitude larger than expected, so called starburst galaxies, and galaxies with no or very little star formation, which are called quiescent galaxies. In this scheme, galaxies are thought to live on the main sequence and gradually grow over time. During their evolution, it sometimes happens that some event triggers a period of intense star formation, for example a merger with another galaxy, during which the galaxy will be in

the starburst phase. When the galaxy grows in mass, the probability grows that something happens that turns off star formation, and when this happens, the galaxy is called quenched.

Two of the outstanding questions in galaxy evolution are what supplies gas to the galaxy through which it can maintain its star formation, and what mechanism is responsible for shutting down star formation. Possible scenarios for the former question include a constant accretion of small clouds of gas (e.g. Kereš et al. 2005; Genzel et al. 2010; Schreiber et al. 2015) and a stochastic merging with other similarly sized galaxies which bring in more gas (e.g. van Dokkum et al. 2010; Ilbert et al. 2013; Moster et al. 2013; Lehnert et al. 2016). The latter question has become more complicated as one of the currently popular theories is that star formation is shut down by preventing the gas to accrete in the first place. In competition with this starvation scheme is a violent removal of gas by either the triggering of an active galactic nucleus (AGN; e.g. Dubois et al. 2013) or of a short period of very high star formation (e.g. Diamond-Stanic et al. 2012).

To understand the evolution of galaxies and the Universe as a whole, it is thus necessary to understand feedback at high redshift. How common are outflows in galaxies at high-redshift when most stars were forming? What are the spectral properties of massive galaxies at $z \sim 3$ where we expect feedback to be the strongest? At what velocity does gas flow out of galaxies, and what does this depend on? Are the interstellar medium (ISM) conditions in regions with active star formation different in the young Universe than in the local Universe?

In this thesis, I study the above questions using spectroscopic observations with observations from state-of-the-art telescopes. I analyse the shapes of the spectroscopic features to determine the strength and occurrence of outflows in galaxies of various masses, and study if the outflow velocity correlates with stellar mass, star formation rate or redshift. Furthermore, I use the recently installed instrument Multi Unit Spectroscopic Explorer (MUSE) on the Very Large Telescope (VLT) to combine spectroscopic observations over a relatively large area with gravitational lensing to search for very low mass galaxies at high redshift and analyse their properties to unprecedented detail.

The remainder of this chapter provides the necessary background to understand this thesis, starting with an introduction on general cosmology. Furthermore, I introduce UV spectroscopy, what we already know about galaxies at high redshift, and gravitational lensing.

1.1 The formation and evolution of galaxies

1.1.1 Cosmology

Cosmic Microwave Background

After the Big Bang, the Universe expanded and cooled as time went on. While at first the photons and baryons were still tightly connected because the mean free path length was very short, they decoupled when the temperature decreased enough. At that moment, 380,000 years after the Big Bang, photons were for the first time able to escape their local volumes. This had two important consequences. First, baryonic fluctuations in the density were not smoothed out on short scales any more, which means that small overdensities could grow through gravitational attraction. These overdensities were already present due to small random fluctuations in the original quantum field, and remained so because DM does not interact through electromagnetic forces. Second, some photons were able to travel far and were not absorbed again. This means that this is the first source of light we could potentially observe. It also means that we cannot observe anything beyond this point through electromagnetic observations.

Through expansion of the Universe, the wavelength of this first light has been increased by a factor of 1100. This means that the black-body temperature at which it is observed, has decreased by a factor of 1100, to a temperature of 2.7 K at present. In 1964, a radio signal was accidently discovered at this wavelength independently by Doroshkevich & Novikov (1964) in the Soviet Union and Penzias & Wilson (1965) in the US. It was later discovered that this radiation came from the photon decoupling, and it was later called the Cosmic Microwave Background (CMB) due to its cosmic origin and appearance at microwave wavelengths.

The CMB has been analysed in great detail ever since, and it has been determined to be homogeneous down to 10^{-5} K. Space missions, such as *COBE, WMAP*, and *Planck*, revealed further details about the radiation, and we have learned much about the evolution of the Universe from this. For example, the CMB is one of the most reliable methods to determine the age of the Universe and the relative abundance of baryons, dark matter (DM), and dark energy (DE). The latest observations of the CMB show that the Universe is 13.8 billion years old and currently consists of 4.9 % baryons, 25.9 % DM, and 69.2 % DE (Planck Collaboration et al. 2015).

The ΛCDM cosmoglogical model

In the now generally accepted Lambda Cold Dark Matter (ΛCDM) model (White & Rees 1978), galactic haloes form from fluctuations in the density field just after the Big Bang. In ΛCDM the Universe consists of the matter responsible for the light we see, but in addition has a "cold" DM and a DE component. The DM is called dark because it only interacts through

gravity and cold because the particles were non-relativistic at the moment of decoupling, and as a result their potential energy at present day is much higher than their kinetic energy. Dark energy is thought to be responsible for the expansion of the Universe, but what it is remains a complete mystery.

In this ΛCDM model, the evolution of galaxies is largely determined by a small number of physical processes, of which we have only a basic understanding. One of these physical processes is the way galaxies accrete their mass, which mostly depends on gravity and is therefore less complicated than for example star formation, which depends strongly on radiative and hydrodynamical physics. Since gravity has an attractive nature, mass contracts to a structure of filaments and nodes, through which galaxies move towards each other. In the ΛCDM model the Universe starts as hot, homogeneous and isotropic, and cools down due to expansion.

In the hierarchical galaxy formation model, a galaxy is formed as a small unit and grows by accreting matter and merging with other galaxies. A natural consequence of this model is that the galaxies that formed first have had most time to grow and are therefore now the most massive galaxies. Additionally, the assembly rate was significantly higher at high redshift than it is today. Smaller galaxies at the present day formed later, and therefore had at a lower assembly rate and less time to grow. Using this idea in combination with a constant baryon fraction ensures that galaxies grow, but also that the content of baryons in galaxies grows.

The Epoch of reionization

When the Universe cooled down, it resulted in hydrogen and helium becoming neutral and therefore opaque to radiation with energies higher than their ionization thresholds. Because we now observe galaxies at large distances and early epochs at frequencies sufficient to ionize hydrogen, the hydrogen must have been reionized. The time at which this reionization occurred is called the "Epoch of reionizatio" (EOR). For cosmological models, it is crucial to understand when the EOR occurred and what the main drivers of this process were. From the latest CMB measurements it was found that the Universe was reionized between $z = 6$ and $z = 10$, and before $z = 10$ the Universe was mostly neutral (Planck Collaboration et al. 2015).

1.2 Physical processes in galaxy evolution

Galaxy formation models predict that massive galaxies can form rapidly at high redshifts (Mo & White 1996), such that the observed evolution in number density and properties of the first massive galaxies put important constraints on galaxy formation models. These predictions have been confirmed by observations that found that massive galaxies are already present at high redshift (e.g. Ilbert et al. 2013; Caputi et al. 2015). The evolution of the

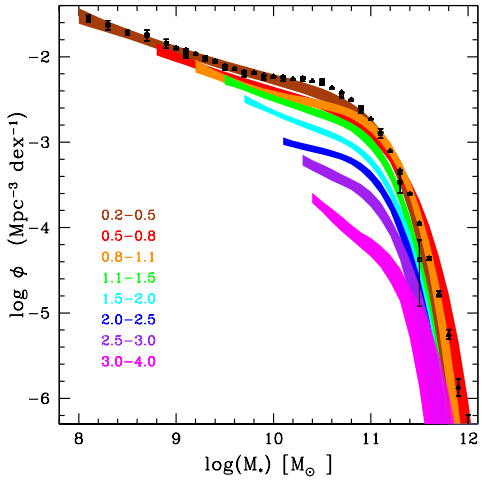

Figure 1.1 – The galaxy stellar mass function at different redshifts shown in different colors (adopted from Ilbert et al. 2013). The stellar mass functions are plotted over the mass range of available data with a width that corresponds to the 68% confidence level. The triangles and squares show the local mass functions found by Moustakas et al. (2013) and Baldry et al. (2012), respectively.

distribution of galaxy stellar masses directly traces the build up of stellar mass in galaxies. The distribution of stellar masses is also called the galaxy stellar mass function (GSMF) and evolves rapidly with redshift (e.g. Ilbert et al. 2013; Muzzin et al. 2013; Caputi et al. 2015); see Fig 1.1.

Galaxy formation models have shown that feedback processes due to star formation and galactic nucleus activity are indispensible to reproduce the observed evolution of the GSMF. In order to create realistic models, galaxy formation models use the GSMF in the local Universe as constraints. when including these constraints, they find that it is necessary to include feedback to explain the early presence of massive galaxies. The rapid change of the GSMF with redshift also implies that the density of star formation in the Universe varied with redshift, which was independently confirmed by observations (see Madau & Dickinson 2014, and references therein). The star formation density increases from at least $z = 8$ to $z \sim 2$, peaks between $1.5 < z < 2$, and decreases afterwards, see Fig. 1.2.

The GSMF at different redshifts is well described by a Schechter function (Schechter 1976). The change in slope in the Schechter function suggests that other different forms of feedback are dominant at stellar masses below and above a certain $M_\star$. Therefore, comparing the presence of an AGN, the amount of star formation (SF), and the effects of feedback in massive to less

massive galaxies provides valuable information about the origin and strength of feedback.

At masses below $M_\star$, most galaxies are found to lie on the"main-sequence of star formation", first suggested by Noeske et al. (2007). This main sequence shows that for a given stellar mass, most of the actively star forming galaxies lie within a relatively narrow range of star formation rates (SFRs). The main sequence extends to high redshift (e.g. Elbaz et al. 2011; Rodighiero et al. 2010; Speagle et al. 2014), although for any given mass an evolution is seen to higher SFRs at higher redshifts. These galaxies form most of their stellar mass on the main sequence, where fuel is provided by a constant stream of smaller galaxies and clumps of gas through the cosmic web.

If the majority of galaxies above $M_\star$ would continue to follow the main sequence of star formation, the clear change of slope in the GSMF would not be seen. When galaxies become more massive, the probability that they become quenched, and therefore not follow the main sequence anymore, increases. The cause of this quenching is still a matter of debate, with possible candidates including AGN feedback (e.g. Dubois et al. 2013), morphological quenching (e.g. Martig et al. 2009), and environmental quenching (for low-mass galaxies, e.g. Peng et al. 2010; Tal et al. 2014). Feedback from SF or AGN are then internal processes that expel gas or heat the surrounding gas, while morphological and environmental quenching are based on the disability of the gas to accrete and cool in the first place. Gas in the inner parts of the galaxy is very low or warm, as studies have shown that star formation is closely correlated with the molecular gas density (e.g. Kennicutt 1998; Leroy et al. 2008; Genzel et al. 2010).

1.2.1 Stellar feedback

Young massive stars produce a strong radiation field in combination with stellar winds. The radiation can ionize the surrounding molecular cloud, creating H II regions around the stars. As a consequence the temperature of the gas increases, but the radiation also exerts a pressure on the dense medium of the cloud. If the pressure is strong enough, it can disperse the dense medium and prevent it from forming more stars. When a massive star collapses at the end of its life, a supernova (SN) is produced. A SN creates a large amount of radiation, but also ejects a large amount of material at high velocity into the ISM. As a result, it is very effective in dispersing the ISM around it. A single star or SN is often not strong enough to disperse the entire region of a molecular cloud, but because stars form in clusters, their combined pressure disrupts the cloud.

When a cloud is disrupted, the gas in and surrounding the cloud can be accelerated to high velocities, which can be high enough to escape the galaxy. Initially, the winds driven by star formation mix with the surrounding gas and deposit the metals formed by the evolution of massive stars. When the winds reach the surface of the disks of galaxies, however, the low density of the circumgalactic medium (CGM) allows the gas to flow more or less freely. If the

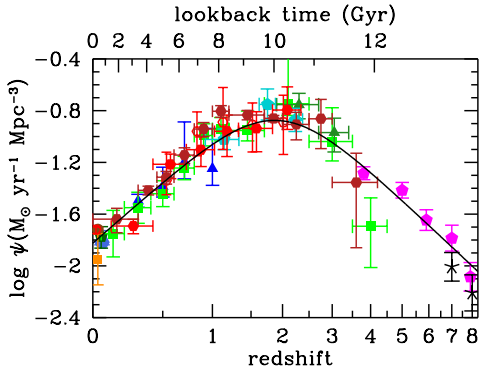

Figure 1.2 – The evolution of the star formation rate density over cosmic time (adopted from Madau & Dickinson 2014). The SFRs have been calculated using a combination of FUV and IR measurements, where every color corresponds to another study. The solid line is the best fit SFRD based on Equation 15 in Madau & Dickinson (2014)

gas still has a large enough velocity, it will escape the gravitational potential well of the gravity and enrich the inter galactic medium (IGM). Otherwise, the gas will be mixed with the CGM and, after cooling down, be reaccreted by the galaxy.

When including feedback directly linked to star formation, galaxies regulate their growth self-consistently, as feedback increases when star formation increases (e.g Schaye et al. 2010). However, the implemented SN feedback was only succesful at masses similar to our Milky Way, while dwarf galaxies formed too much stellar mass and massive galaxies demonstrated too-high star formation rates at $z = 0$. Implementations of new feedback recipes, such as including the effects of the ionizing radiation of young massive stars, and increased resolution have brought recent simulations such as EAGLE (Schaye et al. 2015), NIHAO (Wang et al. 2015), and Illustris (Vogelsberger et al. 2014) into much better agreement with observations.

Because this feedback model directly couples SF to an outflow process, a high SFR causes a higher outflow rate of gas. The high outflow rates have two effects on the gas reservoir. First, the ISM is being heated and pushed out of the galaxy, depleting the gas reservoir. Second, accreting gas finds more resistance when falling into the galaxy and therefore the accrection flow is decreased. Since SF is directly linked to the amount of cold dense gas in a galaxy, it becomes self regulating.

1.3 Properties of galaxies from UV spectroscopy

The GSMF and main-sequence evolution over time point to a difference in the properties of galaxies at fixed mass at different redshifts. Although metallicity might play a role in this evolution, it cannot explain it fully (e.g. Maier et al. 2014; Sanders et al. 2015), and therefore other differences have to be present. Förster Schreiber et al. (2009) showed that the Hα disks of high-redshift star forming galaxies are very different from the disks observed in the local Universe. At $z \sim 2$, the disks are much more clumpy, irregular, and thicker. To understand the gaseous properties of high-redshift galaxies, and consequently the evolution of the stellar component, detailed spectroscopic studies of galaxies are required.

Observations in the optical domain probe the restframe UV emission at $z > 3$. Therefore, the restframe UV has become the most used wavelength range to study the properties of galaxies at high redshift.

The absorption features in the UV spectrum of galaxies have several origins, and their strengths vary with the conditions in the galaxy (e.g. Shapley et al. 2003, and references therein). O IV λ1343 and S V λ1501 originate from the photospheres of stars, and therefore are good lines to determine the galaxy systemic redshift. These lines however, have small equivalent widths, and therefore high-signal-to-noise-ratio (S/N ratio) spectra are required to observe them. Stellar winds cause several absorption features with larger equivalent widths and are therefore easier to detect, but they have higher degrees of ionization and their wavelengths might be shifted with respect to the restframe. N V $\lambda\lambda$1238,1242, Si IV $\lambda\lambda$1393,1402 and C IV $\lambda\lambda$1548,1550 can be caused by stellar winds, but their origin might also lie in the presence of nuclear activity. The stellar wind feature in Si IV is only apparent when there are blue giants or supergiants, while the stellar wind feature in C IV appears for O stars. Shen et al. (2013) show in hydrodynamical simulations that the hot gas surrounding the galaxies is mostly composed of ionized hydrogen, O VI, C IV, Si IV and N V. Observations of these lines in the absence of low-ionization lines therefore indicate a high degree of ionization and that the gas is hot and mostly originating from feedback processes due to star formation and nuclear activity.

The ISM produces the most prominent low ionization features in the UV: see Table 1.1 and Fig. 1.3. Si II 1260, O II 1302, Si II λ1304, C II λ1334, Si II λ1526, Fe II λ1608 and Al II λ1670 are the most obvious FUV absorption lines caused by the neutral ISM (e.g. Shapley et al. 2003; Jones et al. 2012; Talia et al. 2012). Observations of different lines from the same atomic species and energy level, for example Si II, can be used to constrain the conditions of the ISM, as shown by Jones et al. (2013). In addition to the absorption lines, several emission line features can be present in the UV spectra. These emission lines are often originating from H II regions around hot stars, e.g. He II, but can also be the consequence of resonant scattering, e.g. Si II*.

When the profile of absorption lines is spectrally resolved, they can be used to infer kinematic properties of the gas. The width of the line is

Transition	λ_{vac} (Å)	f	Ionization potential (eV)	A/E
H I	1215.67	0.416	13.6	AE
N V	1238.82	0.156	97.9	AE
N V	1242.80	0.078	97.9	AE
Si II	1260.42	1.180	16.3	A
O I	1302.17	0.048	13.6	A
Si II	1304.37	0.086	16.3	A
C II	1334.52	0.128	24.4	A
Si IV	1393.76	0.513	45.1	A
Si IV	1402.78	0.254	45.1	A
Si II	1526.71	0.133	16.3	A
C IV	1548.20	0.190	64.5	AE
C IV	1550.78	0.096	64.5	AE
Fe II	1608.45	0.058	16.2	A
He II	1640.42	0.623	54.4	E
O III]	1660.81	0.000	54.9	E
O III]	1666.15	0.000	54.9	E
Al II	1670.79	1.88	18.8	A
C III]	1906.68	0.000	47.9	E
C III]	1908.68	0.000	47.9	E
Fe II	2249.88	0.002	16.2	A
Fe II	2260.78	0.002	16.2	A
Fe II	2344.21	0.114	16.2	A
Fe II*	2365.66	0.050	16.2	E
Fe II	2374.46	0.031	16.2	A
Fe II	2382.76	0.320	16.2	A
Fe II*	2396.36	0.279	16.2	E
Fe II	2586.65	0.069	16.2	A
Fe II	2600.17	0.239	16.2	A
Fe II*	2612.65	0.122	16.2	E
Fe II	2626.45	0.046	16.2	E
Fe II	2632.11	0.087	16.2	E
Mg II	2796.35	0.616	15.0	AE
Mg II	2803.53	0.306	15.0	AE
Mg I	2852.96	1.830	7.6	A

Table 1.1 – Most prominent UV absorption and emission originating from the ISM. Columns: (1) the atomic line species; (2) wavelength of transition in Å; (3) oscillator strength of transition; (4) Ionization potential of transition; and (5) transition found in absorption (A) or emission (E) in galaxy spectra.

determined by the velocity dispersion in the ISM (interstellar lines) or stars (photospheric lines), while the depth of the line gives the covering fraction at different velocities. A galaxy without inflows or outflows has a symmetrical line profile, best represented by a Voigt profile, so any significant asymmetry is a sign of gas flows. By assuming an ISM of at least two components and fitting the absorption line with the same number of Voigt profiles, the outflow velocity is calculated by measuring the velocity difference between the different components (Weiner et al. 2009; Bordoloi et al. 2014; Bradshaw et al. 2013; Rubin et al. 2014). Additionally, while nebular emission lines or photospheric absorption lines have line centres at zero velocity, the ISM absorption lines can be shifted by the outflow velocity. Restframe UV spectra are therefore often combined with restframe optical spectra to determine the offset of the strong optical emission lines and the UV absorption lines (e.g. Steidel et al. 2010; Erb et al. 2012).

Although it is preferable to use emission lines of the same atomic species and transition to determine the conditions in the ISM, it is possible to use a mix of emission lines to constrain the ionizing source. For example, Feltre et al. (2016) studied the ratios of the most prominent emission lines in the UV for a large range of stellar populations and AGN. From these models, we can then infer whether a set of line ratios is in agreement with a star forming origin, or if more energetic ionizing radiation for an AGN is required.

Emission lines are important for more reasons than simply determining the ionizing source. From their width and profile we can infer the internal dynamics of galaxies while the line ratios of different species can give us the metallicity of the ISM (e.g. Christensen et al. 2012a; Jones et al. 2015). Perhaps most important is that the emission lines have a significantly higher signal to noise ratio than absorption lines. Therefore, emission lines present the only possibility to obtain spectroscopic properties from faint galaxies within a reasonable amount of time.

In addition to line features in the UV, the slope of the UV spectrum (β, defined as $f_\lambda \propto \lambda^\beta$) provides valuable information. Meurer et al. (1999) showed that the dust attenuation at 1600 Å(A_{1600}) depends on β as $A_{1600} = 4.43 + 1.99\beta$. Using this, the intrinsic UV luminosity can be calculated, which provides an estimate for the SFR (Kennicutt 1998)

$$SFR_{UV}(M_\odot \mathrm{yr}^{-1}) = 0.9 \times 10^{-28} \times L_{1500}(\mathrm{erg\ s^{-1}\ Hz^{-1}}). \tag{1.1}$$

Here L_{1500} is the average luminosity of the UV around restframe 1500 Å.

Because restframe (far) infrared observations of sufficient depth are difficult to achieve at high redshifts, determining the dust properties of high-redshift galaxies is challenging. It was shown that β traces the dust properties of galaxies well at low redshift (e.g. Meurer et al. 1997, 1999; Buat et al. 2002) and high redshift (e.g. Seibert et al. 2002; Buat et al. 2012; Reddy et al. 2012; Talia et al. 2015), and is therefore an important observable to probe dust at high redshift. Furthermore, β shows a clear correlation with the total UV

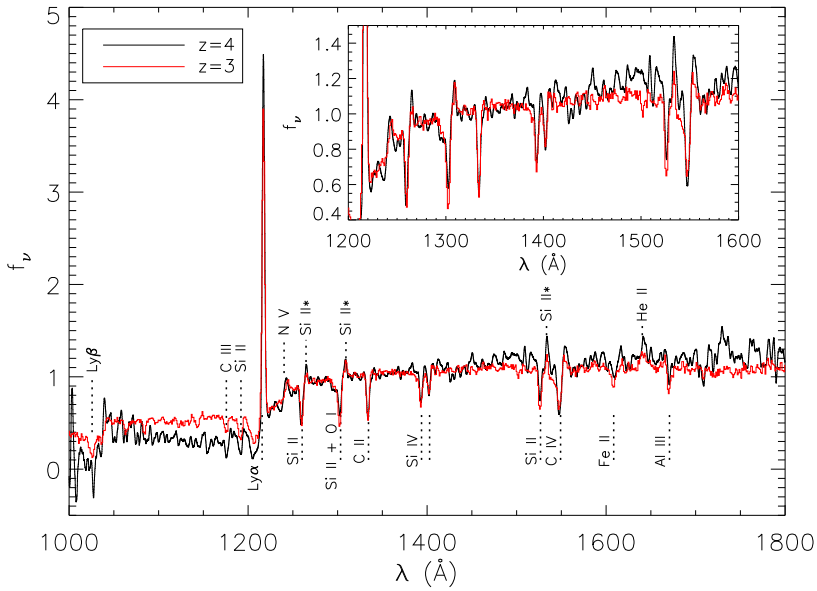

Figure 1.3 – The average UV spectrum of galaxies at $z = 4$ in black and at $z = 3$ in red, obtained after stacking 81 and 811 galaxies respectively. Important UV features are marked by the vertical dashed lines and labels. The figure is adopted from Jones et al. (2012), and the red line shows the result of Shapley et al. (2003).

luminosity (e.g. Bouwens et al. 2009) and age and metallicity of the stellar population.

Although β varies with redshift, this effect is only apparent when not correcting for a changing UV luminosity between $z \gtrsim 4$ and $z \sim 7$, suggesting that galaxies become less massive and less dusty over this period. Recent studies indicate that β decreases with lower stellar mass, flattening at low masses to $\beta \approx -2.2$ to -2.4. Because β is very sensitive to dust and age, it can be used to search for recently formed and pristine galaxies, as these are expected to have very blue continuum slopes $\beta \lesssim -3$ (Leitherer et al. 1999, 2002; Calzetti et al. 2000; Bouwens et al. 2009).

1.3.1 Lyα

The most prominent and important line in the UV is the Lyα line, which corresponds to the energy required to bring a hydrogen atom from the ground state (n=1) to the first excited state (n=2). Because hydrogen is the most abundant species in the Universe and the Lyα cross section is large, only a relatively little amount of neutral gas is needed to completely absorb all photons. In contrast, when the hydrogen has been fully excited or ionized and the radiation field decreases or disappears, the cooling hydrogen will emit a large amount of Lyα photons.

The timescale at which the excited $n = 2$ state in the hydrogen atom falls back to the ground state is orders of magnitude shorter than that of any other transition (Dijkstra et al. 2006). Because of this, Lyα photons are usually absorbed and re-emitted many times before they are able to escape the galaxy into the diffuse IGM. If this were the only relevant process, the fraction of Lyα photons that escape galaxies would be very close to 1, but observations have often shown that only a fraction of Lyα photons escape and most galaxies only show Lyα in absorption. The main reason for this lowering of the escape fraction is dust. Whenever a Lyα photon is absorbed by a dust particle, it can be re-emitted at longer wavelengths through one of the many dust-grain rotational or vibrational transitions. Since the Lyα photons scatter many times within galaxies, their travelled distance is large. Therefore the chance that they are absorbed by a dust particle before they escape the galaxy is large, even when the amount of dust in a galaxy is low. The mean free path length of Lyα photons is therefore an important factor when determining if a Lyα photon can escape a medium, as a longer mean free path decreases the chance of encountering a dust particle.

Recently, several studies have modelled the Lyα radiative transfer in different media to determine how, for example, dust and gas geometry (e.g. Laursen et al. 2013; Gronke & Dijkstra 2016), composition (e.g. Laursen et al. 2011), and gas kinematics (e.g. Verhamme et al. 2006, 2008; Schaerer et al. 2011) in and around galaxies affect the escape of Lyα photons. In general they find that a significant fraction of escaping Lyα photons can be produced through several channels, including the three explained below.

Firstly, because the cross section for Lyα absorption decreases rapidly when moving away from the line center, creating velocity differences in the galactic gas can increase the mean free path of the photons. When a Lyα photon is absorbed by a hydrogen atom which is moving away from the galaxy, it can backscatter the Lyα photon with a longer wavelength. The longer wavelength leads to an energy which is insufficient to excite the hydrogen atoms in the galaxy, and therefore the photon is able to escape the galaxy on the other side. This shift in wavelength leads to the characteristic double-peaked emission lines (Tapken et al. 2007; Verhamme et al. 2008; Gronke et al. 2015): see Chapters 2 to 6 for examples.

Secondly, rather than modifying the velocity of the gas in the CGM, an intrinsic velocity dispersion in the emitting region can help the Lyα photons escape. Similar to the outflowing material, an intrinsic velocity of the emitting atom produces a frequency offset compared to unmoving particles. If the velocity of the emitter is large enough, the mean free path of Lyα will be significantly increased. Therefore, more Lyα photons escape from extended and turbulent H I clouds.

Thirdly, if the CGM distribution is not homogeneous but clumpy, the optical depth becomes dependent on direction. In an ISM or CGM that consists of clumps of dense gas inside a diffuse and hot gaseous halo, Lyα photons scatter off the cloud outer regions, and do not encounter most of the dust which is located inside the dense central regions of the clouds (e.g. Laursen et al. 2013; Gronke & Dijkstra 2014, 2016). In this case, the Lyα photons can escape the galaxy if the gas in the inter cloud medium is either diffuse ($n_{\mathrm{H\,I,ICM}} < 3\times10^{-8}$ cm^{-2}) or the temperature is high (T$\gtrsim 10^6$ K). An additional effect of this geometry is that when the clouds are large compared to the emission region, the optical depth becomes direction dependent, i.e. Lyα photons escape more easily in certain directions. When this occurs, photons will escape in directions with low optical depths more often and the Lyα flux can be boosted in these directions (Laursen et al. 2013; Gronke & Dijkstra 2014).

The shape of the Lyα line profile can be very complex and diverse due to all of the involved parameters, varying from a simple almost Gaussian emission line to triply peaked emission lines with signifant wings on the red and blue sides. Many of these profiles are seen in observations, although some of the more subtle effects require high resolution spectroscopy. The shape of the Lyα line can therefore be very instructive. For example, one can probe the velocity of the outflowing gas by looking at the velocity difference in peaks while a measurement of the flux in the trough between two peaks can constrain the column density. By simultaneously varying several properties and carefully comparing the simulated profiles to observational ones, it is therefore possible to discover the gaseous properties of galaxies (e.g. Verhamme et al. 2006, 2008; Tapken et al. 2007; Dijkstra et al. 2006; Laursen et al. 2009, 2011, 2013; Schaerer et al. 2011; Gronke & Dijkstra 2014; Gronke et al. 2015; Gronke & Dijkstra 2016).

Although we now understand relatively well that a low column density, a high outflow velocity, and a high degree of ionization are beneficial to the escape of Lyα photons, observations have still not resolved what stellar parameters are connected to a galaxy becoming a Lyα emitter (LAE) or not. Some of the difficulties are that the small amounts of H I in the Milky Way and the local Universe absorb almost all Lyα photons coming from the local Universe and that the Earth atmosphere is opaque to UV photons. As a result, the regions which emit Lyα photons can only be spatially resolved with space telescopes, or through gravitational lensing.

Because of the observational difficulties of Lyα in the low redshift Universe, LAEs have been mostly studied at $2 < z < 4$, although the addition of the Cosmic Origins Spectrograph (COS) to *HST* allowed for low redshift Lyα studies like the Lyα Reference Sample (LARS; Östlin et al. 2014). The high-redshift studies have revealed a rapid evolution of the importance of LAEs, where the fraction of LAEs increases quickly with redshift out to $z \sim 6.5$ (e.g. Ouchi et al. 2008; Cassata et al. 2011, 2015; Pentericci et al. 2011; Curtis-Lake et al. 2012; Schenker et al. 2012; Henry et al. 2012). This evolution is faster than the evolution of the star formation density of the Universe, and suggests therefore an intrinsic evolution of galaxy properties over this period. The fraction of LAEs is higher at lower metallicity, higher ionization-degree, and lower dust mass, both at low (e.g. Cowie et al. 2011; Hayes et al. 2014) and high redshift (e.g. Erb et al. 2010; Blanc et al. 2011; Nakajima et al. 2012; Guaita et al. 2013). Additionally, the evidence is building that the fraction of LAEs decreases with increasing stellar mass (Dijkstra & Gronke 2016; Oyarzún et al. 2016). As the average stellar mass, dust mass, and metallicity increase with time, the quick evolution of the fraction of LAEs is only expected, and illustrates the importance of the Lyα line for gaining a better understanding of the local Universe.

The increased fraction of LAEs at high redshift and low stellar masses provides a fortunate opportunity, as this gives us a chance to study the properties of low mass galaxies at high redshift. Without this imporant emission line, the faintness of these galaxies would largely hamper the possibility of determining spectroscopic redshifts for this population of galaxies. Consequently, without Lyα it would be very difficult to deduce any properties from spectroscopy for all but the brightest galaxies.

Because Lyα is a resonant line the photons scatter often through the gaseous medium. Therefore, Lyα emission can be extended compared to the light coming from the stars as it comes from where it was last scattered. Up to $\lesssim$ 80 kpc there is enough hydrogen (e.g. Steidel et al. 2010) for Lyα to be scattered, although the surface flux density is often too low to be detected (but see Steidel et al. 2011, for a detection of extended emission using stacking). Carefully measuring the extent and the profile of the Lyα surface brightness therefore provides a powerful method to measure the density of gas surrouding galaxies.

1.3.2 Detecting gas flows

As shown above, the pace of galaxy growth peaks around $z \sim 2-3$, which suggests that galaxies have been more efficient in star formation at these redshifts or had much more gas available to form stars. The higher gas accretion rates than found locally could be due to a higher merger rate of galaxies, as is expected at higher redshifts, or due to a more efficient mechanism for transporting cool gas to the center of galaxies. Kereš et al. (2005), Genzel et al. (2008) and Dekel et al. (2009), among others, suggested that at high redshifts the gas does not always heat when it enters the galaxy due to virialization, but that cold streams can also develop which bring the cold gas directly to the centers of galaxies. It is unlikely that only one of these mechanisms is responsible for the higher assembly rates, but to date there is no clear evidence for cold streams in observations, and some simulations contradict these results (e.g. Klar & Mücket 2012).

Pettini et al. (2001) show that there is, on average, a systematic shift in interstellar (IS) lines in the UV and the photospheric lines in the optical restframe of LBGs of several hundreds of kilometers per second. Since the stars are moving along radial or elliptical orbits, they are at rest in galaxies, such that they are a good measure of the galaxy's systemic redshift. The difference between the interstellar lines and the stellar lines is therefore due to a motion of the interstellar gas. If the IS lines are blueshifted with respect to the systemic redshift, it means that the interstellar gas has an outwards motion, while a redshift will be due to inflowing gas. From this shift it is thus possible to detect inflows and outflows in a galaxy, and to estimate the velocity at which this is happening.

Steidel et al. (2010) confirmed the results of Pettini et al. (2001) by studying a sample of LBG galaxies with UV spectra. In addition they use projected galaxy pairs to study the CGM. These projected pairs consist of one galaxy in the background of another galaxy, with a small angular separation. The light emitted by background galaxy then travels through the CGM of the foreground galaxy, and absorption features from this CGM can then be seen in the spectrum of the background galaxy at the redshift of the foreground galaxy. The width of these features is used to estimate the velocity at different distances from the galaxy, and they find that at 80 kpc material is flowing outwards at 800 km s^{-1}. The model they fitted to their data has an increasing velocity with distance, since the radiation from the galaxy accelerates the outflowing material. Although outflows have been discovered by many different teams in various galaxies (e.g. Martin 2005; Martin et al. 2012; Rupke et al. 2005a; Weiner et al. 2009; Bordoloi et al. 2014; Erb et al. 2012; Bradshaw et al. 2013; Rubin et al. 2014), very few observations of possible inflows have been reported (e.g. Bouché et al. 2013).

1.3.3 Analogues of EOR galaxies

Current studies indicate that low-mass galaxies produced a significant fraction of the photons that reionized the Universe (Wise et al. 2014; Kimm & Cen 2014; Robertson et al. 2015, but see Sharma et al. 2016). However, it is still observationally unfeasible to directly observe these faint galaxies with existing telescopes, which has led to a search for analogues of these galaxies. Galaxies between $z = 3 - 6$ are observationally easier to observe, due to their smaller distance from us and the lack of obscuration due to the neutral IGM, while their ISM conditions are closer to reionizing galaxies than local analogues. In addition, the density of low-mass, intensively-star-forming galaxies is very low in the local Universe, which makes it very difficult to find a significant number of local analogues.

At $z \sim 3$, there have now been several studies which tried to determine the fraction of ionizing photons that can escape a galaxy. So far, the success rate of these studies has been very low, and often only upper limits for the escape fraction of Lyman continuum (LyC) photons (f_{esc}) have been set. Recently, some authors (de Barros et al. 2016; Izotov et al. 2016) discovered that galaxies with extremely high emission line fluxes have non-zero LyC emission. Studying these sources at high and low redshift is therefore a promising strategy to understand what is responsible for this emission, and combining their properties with luminosity and number density functions will confirm or reject these galaxies as main drivers of reionization.

As explained above, the escape of Lyα photons depends on the H I column density. Because the escape of LyC photons requires low column densities $N_{\mathrm{H\,I}} \lesssim 10^{17}$ cm^{-2}, there is a correlation between the escape fraction of Lyα and LyC photons (Dijkstra & Gronke 2016). In addition to this, outflows and stellar winds can create bubbles in the ISM and CGM of very low density gas. Therefore, the escape of LyC photons could be helped further through feedback processes in LAEs. As a result, LAEs can be used to look for LyC emitting galaxies using the shape of the Lyα line to select low column density sources. Narrow Lyα lines and a small velocity difference between the red and the blue peak are therefore good indicators of LyC candidates (e.g. Vanzella et al. 2016a). Additional features in the UV spectrum, such as narrow absorption lines (Jones et al. 2013) or narrow UV emission lines (Vanzella et al. 2016a), provide additional evidence for a low column density.

1.4 Gravitational lensing

In the theory of general relativity mass bends space and time. As a consequence, when light passes close to a large mass, it is deflected. The possibility of light being deflected by mass was first discussed by John Mitchell in 1784 and Johann von Soldner in 1804 before general relativity was invented. The effect is similar to what happens when an optical lens focusses the light

at a certain distance, although without any focal length, and it is therefore called gravitational lensing. The details of general relativity which make this effect possible are beyond the scope of this thesis but see Blandford & Narayan (1992); Refregier (2003); Van Waerbeke & Mellier (2003); Schneider (2006) and Treu (2010) for excellent reviews on gravitational lensing. Here I only give a short description to understand processes relevant in this thesis.

Gravitational lensing is observed at different mass and distance scales, from single stars (microlensing) to clusters of galaxies. The deflection caused by gravitational lensing depends on distance of the path of the light in the source plane (ξ), the total enclosed mass of the lens within a radius ξ from the lens centre, and the relative distances of the source and the observer to the lens. By measuring the distances to lens and source and determining the deflection angle and ξ, it is therefore possible to derive the total mass of the lens. Although the physics of gravitational lensing are the same, it is often separated into three regimes. The first is strong lensing (SL), where the deflection of light is relatively strong (although still small in absolute numbers, e.g. Kochanek 2006), the second is weak lensing (WL), where the deflection angle and magnification are relatively small, and the third is microlensing.

The most prominent regime is SL, which has several important consequences and uses in astronomy. If a source is well aligned with an (almost) axisymmetric lens and the observer, the light can travel in any direction around it, and consequently create an "Einstein ring". If the source is slightly offset, there will still be multiple paths around which the light can travel to reach the observer, and multiple images of a source can be detected around the center of the lens. The number of multiple images can vary and depends on the position of the source and the exact geometry of the lens.

In the case of multiple images, the path length of each image can be different, because the light paths pass the lens plane at different distances from the source and therefore have different deflection angles. This increased path length can be balanced or even countered by Shapiro delay (Shapiro 1964), which states that light passing close to a mass moves slower. By measuring the difference of the arrival time of photons, one could securely study the lens properties, but also cosmological parameters (e.g. Refsdal 1964; Treu et al. 2016).

In WL, only mild magnifications are found, and the most important effect is the distortion of background sources in the tangential direction. Detecting objects affected by WL is more difficult than with SL, as many galaxies are elongated by nature and many foreground objects will therefore confuse the selection. However, while the orientation of foreground galaxies is random, the WL distortion is tangential, and WL can therefore be detected in a statistical way by looking at the average orientation of galaxies.

Microlensing occurs when a moving mass intersects the path of a background source (e.g. Alcock et al. 1993; Sumi et al. 2011). Examples of microlensing are the brief but significantly increased magnification of stars in

nearby galaxies by stars in our galaxy, or a dark matter overdensity in the halo of a lensing galaxy that magnifies the background object while moving in front of it.

In parts of this thesis, we use SL to probe faint galaxies which are otherwise currently unaccessible. We use a cluster of galaxies which magnifies background galaxies by factors of $\sim$ 5 to $\sim$ 50, and thereby allow us to probe several magnitudes deeper than in fields without strong lensing. In particular, we combined our integral-field spectroscopy with photometric observations from the Frontier Fields Programme (FF; Lotz et al. 2016; Koekemoer et al. 2016). The FF programme consists of multi-wavelength deep *HST* imaging towards 6 galaxy clusters with SL, which have been selected based on their lensing strength, sky darkness, *Spitzer* and *James Web Space Telescope* observability, and pre-existing ancillary data. The imaging is done in 7 different filters spanning from the B-band through the H-band, and reaches a 5σ depth of 28.5-29.1 AB magnitudes in all filters. This depth is necessary to reach the goals of the FF programme, which are focussed on revealing and studying galaxy populations at high redshift which have otherwise been unaccessible. These are therefore the deepest observations of gravitationally-lensing clusters and their lensed backgrounds to date.

Although the aim of this thesis is not to reconstruct the lens models and study the clusters themselves, spectroscopic observations of high-redshift galaxies automatically provide constraints for the lens model. These constraints result from the redshifts of sources and lens, which determine their distances. In addition, the separation of images is directly related to the deflection angle, and therefore all necessary information is available to determine the mass of the lens within a radius, if the lens is axisymmetric. Unfortunately, galaxy clusters are not axisymmetric, but they can be approximated by a linear combination of elliptical masses.

The bulk of this thesis consists of the spectroscopic analysis of high-redshift galaxies, for which I have been the main contributor. In Chapter 6 I performed the spectral analysis, which plays an important role in the gravitational lens construction, while the lens reconstruction itself was performed by my collaborators. Chapter 6 is included because it contains an important spectroscopic effort and to demonstrate the reconstruction of the FF gravitational lens MACS1149 with a large number of observations and constraints. In Chapters 4, 5, and 7 we use the outcome of similarly constructed lensing models, which are updated and better constrained with the used observations. For example, in Chapter 5 we used the predicted magnification factors for the FF cluster AS1063 to spectroscopically and photometrically study the properties of the intrinsically faintest galaxies observed to date. The multiple images of the observed galaxies help to constrain the properties of these galaxies, and provide an independent check of the derived magnification values.

1.5 This thesis

The subject of this thesis is the study of different physcial properties of galaxies at $z > 2.5$ when the Universe was less than 2.5 Gyr old, in particular the occurence of outflows in these galaxies. For this, we analyse data from state-of-the-art optical spectrographs. We aim to determine how different ISM characteristics are related to galaxy propreties like stellar mass and SFR. At these redshifts, the Universe was in its most active phase, with the star formation density rising and black hole accretion rates to their peaks at $z = 2 - 3$. According to current galaxy evolution models, this should be accompanied by large quantities of gas flowing out of the galaxies. It is still uncertain, however, how common these outflows are, or how strong they are.

Outflows can be measured with spectra of sufficient resolution and depth to separate the different kinematical components of the ISM. In Chapter 2 we perform deep observations of a sample of 11 galaxies at $z \sim 3$. These galaxies were selected to be massive and bright in the restframe UV, such that our deep and relatively high-resolution spectroscopic observations have a high S/N ratio. Using these spectra, we model the shape of the UV absorption lines to study the prevalence of outflows and measure the outflow velocities in these objects.

In Chapters 3, 4, and 5 we use the MUSE integral field spectrograph to observe the gravitationally-lensed background of galaxy cluster AS1063. In Chapter 3, we present the quality of the data, the data reduction process, and a catalogue of $\sim$ 60 galaxies with spectroscopic redshift determinations. In addition, we study the individual spectral properties of a number of interesting objects. Chapter 4 focusses on the discovery of an extended Lyα nebula discovered by these observations. We discuss the extent of the nebula, as well as the origin of the ionizing radiation. In Chapter 5, we discuss the properties of the discovered LAEs behind AS1063. These objects are amongst the faintest galaxies studied at any redshift to date. Therefore, studying their properties is necessary to understand the building blocks of the more massive galaxies seen today.

Chapters 6 and 7 focus on the discovery of the multiply imaged SN Refsdal. We use MUSE observations to build a more accurate gravitational lensing model, and describe this in Chapter 6. This improved model is necessary to make predictions for the reappearance of the SN. Chapter 7 is a study on the ISM conditions where SN Refsdal exploded. The combination of MUSE and gravitational lensing leads to and unprecedented combination of spatial and spectral resolution at $z = 1.5$. Finally, in Chapter 8 I present my conclusions and give a brief outlook of possible research in this field.